Transparent resistive switching memory using aluminum oxide on a flexible substrate

2016 Nanotechnology 27 07LT01

(http://iopscience.iop.org/0957-4484/27/7/07LT01)

IOP Publishing
Letters
Nanotechnology
Nanotechnology 27 (2016) 07LT01 (6pp)
doi:10.1088/0957-4484/27/7/07LT01

Letter

Transparent resistive switching memory using aluminum oxide on a flexible substrate

Seung-Won Yeom[1], Sang-Chul Shin[2], Tan-Young Kim[1], Hyeon Jun Ha[1], Yun-Hi Lee[3], Jae Won Shim[2,4] and Byeong-Kwon Ju[1,4]

[1] Display and Nanosystem Laboratory, College of Engineering, Korea University, Anam-dong, Seoul 139-713, Korea
[2] Department of Electronic and Electrical Engineering, Dongguk University, Seoul 100715, Korea
[3] National Research Laboratory for Nano Device Physics, Department of Physics, Korea University, Seoul 136-713, Korea

E-mail: jwshim@dongguk.edu and bkju@korea.ac.kr

Received 16 November 2015, revised 8 December 2015
Accepted for publication 17 December 2015
Published 14 January 2016

Abstract

Resistive switching memory (ReRAM) has attracted much attention in recent times owing to its fast switching, simple structure, and non-volatility. Flexible and transparent electronic devices have also attracted considerable attention. We therefore fabricated an Al_2O_3-based ReRAM with transparent indium-zinc-oxide (IZO) electrodes on a flexible substrate. The device transmittance was found to be higher than 80% in the visible region (400–800 nm). Bended states (radius = 10 mm) of the device also did not affect the memory performance because of the flexibility of the two transparent IZO electrodes and the thin Al_2O_3 layer. The conduction mechanism of the resistive switching of our device was explained by ohmic conduction and a Poole–Frenkel emission model. The conduction mechanism was proved by oxygen vacancies in the Al_2O_3 layer, as analyzed by x-ray photoelectron spectroscopy analysis. These results encourage the application of ReRAM in flexible and transparent electronic devices.

Keywords: resistive switching, ReRAM, oxygen vacancy, Poole–Frenkel emission

(Some figures may appear in colour only in the online journal)

1. Introduction

Flexible electronic devices on plastic substrates have been popular in recent times because of their slimness, light weight, and human-friendly interfaces compared to conventional bulk silicon devices. They are employed in a variety of electronic devices such as e-paper [1], flexible solar cells [2], and flexible displays [3]. In addition, transparent electronic devices are potentially applicable in other devices such as transparent transistors [4] and diodes [5]. This has increased the need for flexible and transparent memories. A flexible and transparent memory is expected to become an important part of electronic devices for data processing, storage, and communication. Flexible and transparent memories will therefore contribute to the development of future electronic systems.

Current silicon-based flash memories consisting of a metal-oxide-semiconductor field-effect-transistor with an additional floating gate in each memory cell need to be scaled down to increase their data storage capacity. However, flash memories are expected to reach their scaling limitation in the near future [6]. Extensive efforts are thus being made to develop the next generation of memory devices such as ferroelectric random-access memory (FeRAM) [7], magnetic random-access memory (MRAM) [8], phase-change random-access memory (PCRAM) [9], and resistive switching memory (ReRAM). Among these different memories, ReRAM is the most promising candidate for the next generation of

[4] Author to whom any correspondence should be addressed.

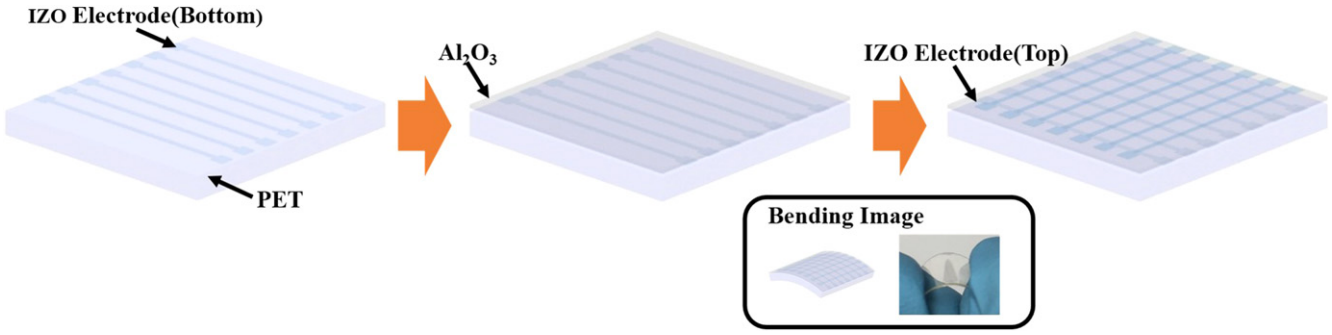

Figure 1. Schematic of the process flow for fabricating the FT-ReRAM device. The inset shows the bended FT-ReRAM.

memories owing to its simple metal–insulator–metal structure, non-volatility, quick switching, good endurance, and long retention time [10, 11].

Towards achieving better ReRAM characteristics, various studies have been conducted to investigate resistive switching phenomena in different materials [12]. Metal oxides such as Ta_2O_5 [13], ZrO_2 [14], Cu_2O [15], TiO_2 [16], and Al_2O_3 [17] in particular have received much attention for use in fabricating ReRAMs because of their good compatibility with semiconductor manufacturing technologies and low-cost fabrication. Among these materials, Al_2O_3 has promising characteristics such as resistive switching properties, as well as their wide band gap, large breakdown electric field, high permittivity, and good thermal stability. These properties have prompted the common use of the material as a gate dielectric insulator in thin-film transistors [18] and an encapsulation layer in organic devices [19]. Al_2O_3 can thus be used in flexible and transparent ReRAMs (FT-ReRAMs) while maintaining its resistive switching properties.

The use of a flexible and transparent electrode is essential for the fabrication of an FT-ReRAM. Currently, the most widely used transparent electrode is indium–tin oxide. Unfortunately, this material is very brittle and susceptible to cracking, and this makes it unsuitable for use as a flexible and transparent electrode. It is therefore necessary to consider more robust transparent electrodes that remain stable when flexed. In this study, we used a stable amorphous indium–zinc oxide (IZO) electrode with a smooth surface, high transmittance, and good flexibility [3].

In this study, we fabricated simple all-sputtered FT-ReRAM (IZO/Al_2O_3/IZO) devices on flexible PET substrates at room temperature. The electrical properties of the devices were examined, and low-voltage operation ($\pm$3.2 V), high a on–off ratio (near 10^3), good retention (10^5 s), and endurance (10^3 cycles) were observed. The transmittance and flexibility of the devices were investigated. The devices exhibited higher than 80% transmittance in the visible region (400–800 nm), good endurance, and long retention even under bended states (radius = 10 mm). In addition, the conduction mechanisms of the Al_2O_3-based devices were examined based on the oxygen vacancies to verify their suitability for FT-ReRAM applications. Ohmic conduction and a Poole–Frenkel emission model were employed for this purpose. The proposed FT-ReRAM devices may be useful for the development of next-generation portable equipment and are worthy of further study.

2. Experiment

The proposed all-sputtered FT-ReRAM (IZO(250 nm)/Al_2O_3(40 nm)/IZO(250 nm)) sandwiched structure on a commercial PET substrate was fabricated as shown in figure 1. The inset in figure 1 shows the bended FT-ReRAM. The 250 nm thick bottom IZO electrodes were deposited using a radio frequency (RF) sputtering method at room temperature and a metal shadow mask composed of eight lines (each 60 μm wide) directly above the flexible PET substrate. No silicon wafer or glass substrate was used for mechanical support. The sputtering was carried out in ambient pure Ar plasma supplied at 3 sccm with a power of 150 W and a working pressure of 4 mTorr. To fabricate the insulating layer, a 40 nm thick Al_2O_3 film was subsequently deposited by RF sputtering at room temperature. The sputtering of the insulating layer was performed in ambient pure Ar plasma supplied at 4 sccm with a power of 150 W and a working pressure of 4 mTorr. Next, the top 250 nm thick IZO electrode was deposited vertically to form a crossbar structure with an 8×8 array. This was done by the same method used to deposit the bottom electrode. X-ray photoelectron spectroscopy (XPS) measurement was performed using a ULVAC-PHI X-tool. The electrical characteristics were measured using a Keithley 4200 semiconductor parameter analyzer. During these measurements, a bias was applied to the top electrode while the bottom electrode was grounded. All the measurements were performed at room temperature.

3. Results and discussion

Figure 2(a) shows the optical transmittance spectra of the FT-ReRAM obtained using a UV–visible spectrophotometer. The spectra indicate that the transmittance of the FT-ReRAM was higher than 80% in the visible region (400–800 nm wavelength). This was because of the transparent IZO electrodes of the device, the wide band gap of the thin Al_2O_3 layer, and the transparent PET substrate. The logo of DIANA Lab can be clearly seen under the FT-ReRAM device in the inset in

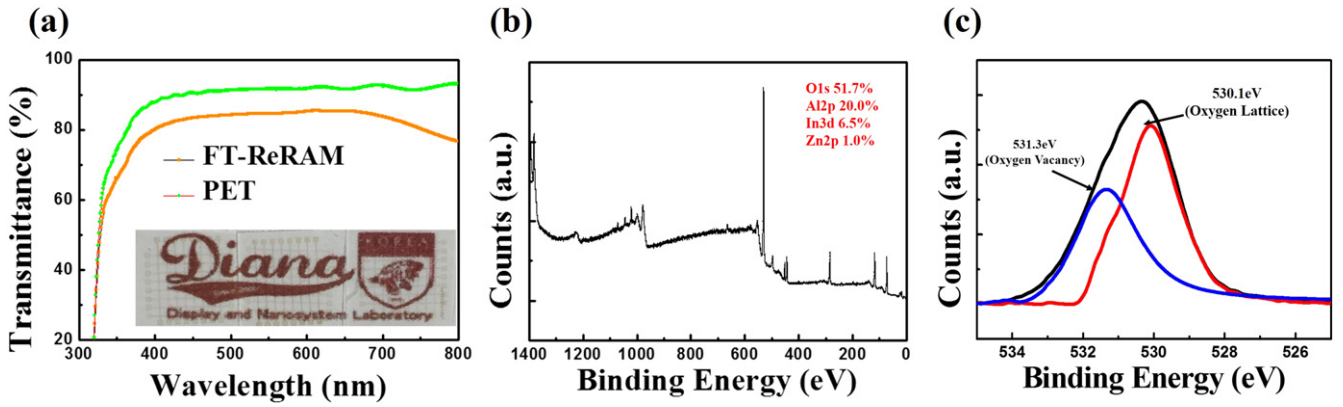

Figure 2. (a) Optical transmission spectrum of the FT-ReRAM. The inset shows a photograph of the FT-ReRAM device above the DIANA Lab logo. (b) XPS survey scan of the FT-ReRAM. (c) O 1s spectra of the FT-ReRAM.

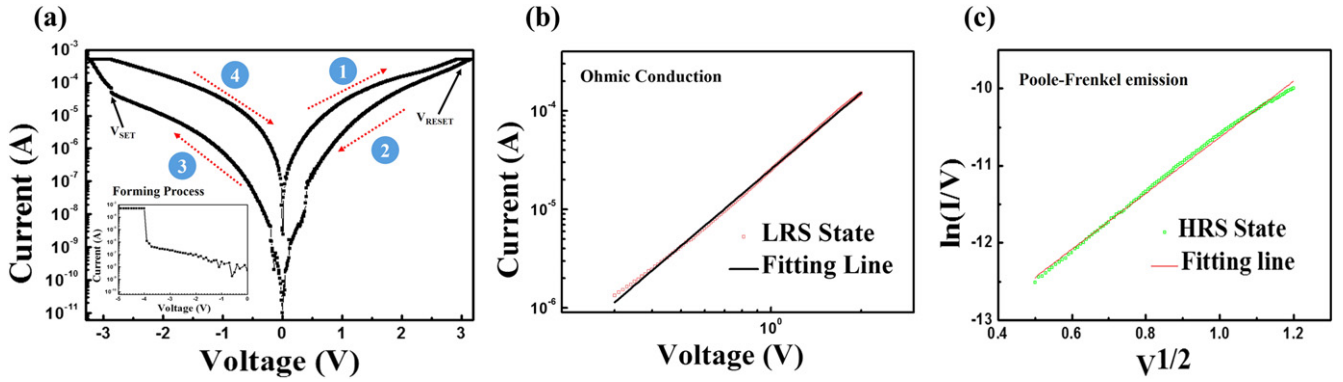

Figure 3. (a) Typical bipolar *I–V* curve of the FT-ReRAM device. The inset depicts the formation process of the FT-ReRAM cell. (b) Log–log scale *I–V* curve in the LRS (used to explain the ohmic conduction). (c) $\ln(I/V)$ versus $V^{1/2}$ curve (used to explain the Poole–Frenkel emission).

figure 2(a). The obtained results confirm that our device can be used as a transparent ReRAM. To verify the IZO/Al_2O_3/IZO structure, the In, Zn, Al, and O components were analyzed by XPS, the results of which are shown in figures 2(b) and (c). Figure 2(b) shows the XPS survey scan of the IZO/Al_2O_3/IZO device. The elemental composition of the FT-ReRAM was determined by energy dispersion. The results in figure 2(b) indicate that our FT-ReRAM comprised 51.7% O, 20% Al, 6.5% In, and 1% Zn. The O 1s spectra from the Al_2O_3 layer are depicted in figure 2(c). They were fitted by their Gaussian components at 530.1 and 531.3 eV. The XPS analysis of the Al_2O_3 layer revealed an asymmetric O 1s spectra from the Al_2O_3 layer that could be deconvoluted into two peaks, as shown in figure 2(c). The binding energy at 530.1 eV can be attributed to the oxygen that was bound to the Al_2O_3 layer lattice, while that at 531.3 eV can be attributed to oxygen deficiencies (oxygen vacancies) in the Al_2O_3 layer. Several previous studies have established a correlation between non-lattice oxygen and the formation of oxygen vacancies [20, 21]. Therefore, issues related to oxygen vacancies are discussed at the end of this paper. The typical resistive switching phenomenon of the FT-ReRAM cells was investigated using the *I–V* curve and a dc voltage sweep. During all the measurements, the bottom electrode was grounded and a bias was applied to the top electrode. It was necessary to first apply a forming voltage to the FT-ReRAM because the device was initially in the high resistance state (HRS) of the as-deposited condition. When a negative bias voltage (0 to −5 V) was applied, an abrupt increase in the current was observed at approximately −4 V (V_{Forming}), as shown in the inset to figure 3(a). A compliance current of 500 μA was imposed during the forming and set processes to prevent breakdown of the device by the abrupt increase in current during switching. The forming process was essential for activating the FT-ReRAM and converting it from the HRS to a low resistance state (LRS). Subsequently, the *I–V* properties of the FT-ReRAM structure were determined by voltage sweep measurements in the sequence 0 V → 3.2 V → 0 V → −3.2 V → 0 V. Before applying the specific positive voltage (V_{RESET}), the current was maintained in the LRS. However, the device was converted from the LRS to the HRS above the specific positive voltage of 3 V. Likewise, before the application of the specific negative voltage (V_{SET}), the device was maintained in the HRS. However, after the application of the specific negative voltage to the FT-ReRAM, the device was converted from the HRS to the LRS. To investigate the switching mechanism of the Al_2O_3-based FT-ReRAM device, the *I–V* curves were replotted in the LRS and HRS. First, to determine the conduction mechanism in the LRS, we replotted a double logarithmic scale graph for the

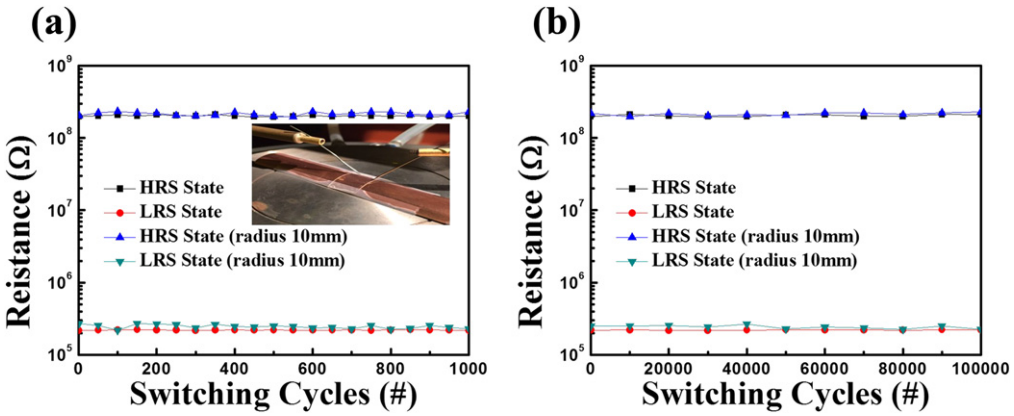

Figure 4. (a) Endurance characteristics of the FT-ReRAM in the flat and bended states, respectively, measured at $V_{READ} = -0.1$ V. The inset shows the measurement set-up for the bending test. (b) Results of the retention tests of the FT-ReRAM in the flat and bended states.

LRS before the application of the V_{RESET}. Figure 3(b) shows a linear slope with a gradient of approximately 1, which confirms that the conduction mechanism in the LRS is dominated by ohmic conduction [22]. Furthermore, we used Poole–Frenkel emission to examine the conduction mechanism of our FT-ReRAM in the HRS. Poole–Frenkel emission, which is the conduction of electricity by an electrical insulator, is characterized by the following equation: [23]

$$\ln\left(\frac{I}{V}\right) \approx \left[\left(\frac{q^3}{\pi d \varepsilon_r \varepsilon_0}\right)^{\frac{1}{2}}\right]\frac{V^{\frac{1}{2}}}{k_B T},$$

where q is the electric charge, d is the film thickness, ε_r is the dynamic dielectric constant, ε_0 is the permittivity of free space, k_B is Boltzmann's constant, and T is the absolute temperature. According to the Poole–Frenkel emission equation, the current characteristics can be analyzed in terms of the relationship between $\ln(I/V)$ and $V^{1/2}$, which can be used to determine the dominant conduction mechanisms [22–24]. By replotting the data in the form of $\ln(I/V)$ versus $V^{1/2}$, as shown in figure 3(c), the conduction mechanism can be well fitted to the Poole–Frenkel emission in the low-voltage region in the HRS.

Next, to examine the reliability and non-volatility of the FT-ReRAM device, we measured the endurance and retention at room temperature, including in the bended state using a bending radius of 10 mm. The inset in figure 4(a) shows the measurement set-up. Figure 4(a) shows the endurance test results for the IZO/Al_2O_3/IZO FT-ReRAM cell. The reading voltage after the set and reset processes was −0.1 V. The resistances in both states were more distributed, especially for the bended FT-ReRAM device. However, the on–off ratio was sufficient to extinguish the states of the FT-ReRAM. One thousand cycles of switching between the HRS and LRS were successfully performed on our FT-ReRAM device, including after bending. This endurance test confirmed the excellent reliability of our device under bended states. The retention characteristics were also examined in both the flat and bended states (bending radius of 10 mm). As shown in figure 4(b), the current was measured at a voltage of −0.1 V every 10^5 s. The resistances in both states under bending were slightly distributed. However, the fluctuations of the resistances were sufficient to dissolve both states. Good non-volatility was observed even after 10^5 s. The results of the endurance and retention tests indicate that the performance of our FT-ReRAM is not affected by bending. This is because of the good flexibility of the two IZO electrodes and the thin Al_2O_3 layer.

Previous studies on metal-oxide-based ReRAMs have shown that the switching mechanism is dominated by oxygen vacancy generation and recombination [11, 24–26]. The resistive switching phenomena can therefore be presumed to be due to oxygen vacancies in the Al_2O_3 layer. From the results of the Poole–Frenkel emission examination, we observed that oxygen vacancies in the Al_2O_3 layer acted as traps for injected electrons, as shown in figure 5. As shown in figure 5(a), during the set process, when a negative voltage was applied to the top electrode, the oxygen ions were removed from the lattice, leaving vacancies in the Al_2O_3 layer. The formation of the oxygen vacancies can be described using the Kroger–Vink notation as follows: [27, 28]

$$O_o \rightarrow V_o'' + 2e^- + (1/2)O_2$$

where V_o'' denotes an oxygen vacancy with a double positive charge in the regular lattice, and O_o denotes an oxygen ion in a regular site. Oxygen ions drift towards the IZO/Al_2O_3 interface and are stored there. This process led to the formation of conductive filaments in the Al_2O_3 layer. In contrast, when a positive voltage was applied to the top electrode, as shown in figure 5(b), the oxygen ions migrated from the interface and filled the vacancies, resulting in the rupture of the conductive filaments in the Al_2O_3 layer.

We therefore believe that the resistive switching in our FT-ReRAM is associated with the ionic migration of oxygen ions, which leads to the formation of oxygen vacancies, and consequently an Al_2O_{3-x} layer on the pristine layer, as shown in figure 5(a). This changes the FT-ReRAM cell resistance to the LRS state. Conversely, during the reset process, the oxygen ions migrate back to the Al_2O_{3-x} layer, resulting in the reformation of the Al_2O_3 layer, as shown in figure 5(b). This causes the FT-ReRAM cell resistance to revert back to the HRS state.

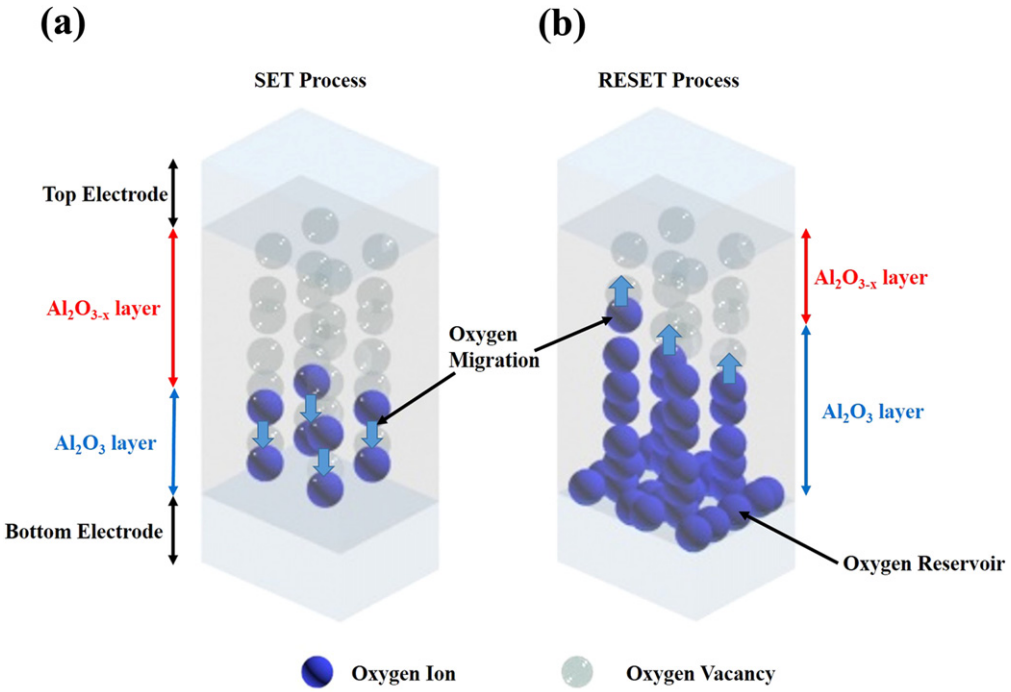

Figure 5. Schematics of the FT-ReRAM during the (a) set and (b) reset processes.

4. Conclusions

We fabricated a simple all-sputtered FT-ReRAM (IZO/Al_2O_3/IZO) for use in next-generation electronic devices. The FT-ReRAM is characterized by a good on–off ratio, low-voltage operation, and good flexibility and transparency. The device also exhibits excellent endurance and long retention, including under bending, owing to the high flexibility of its IZO electrodes and the thin Al_2O_3 layer. The conduction mechanism of the resistive switching device was explained by ohmic conduction and Poole–Frenkel emission. The elemental composition of the FT-ReRAM was also analyzed using XPS analysis. The FT-ReRAM was found to have a transmittance of higher than 80% in the visible region (400–800 nm). We believe that the present work will contribute to the development of next-generation flexible and transparent memory devices.

Acknowledgments

This work was supported by the KSSRC program (Stretchable Multi Sensor for Wearable IoT Device), and partially by the Industrial Strategic Technology Development Program (10045269, Development of Soluble TFT and Pixel Formation Materials/Process Technologies for AMOLED TV) funded by MOTIE/KEIT. The work was also supported by the 2015 Dongguk University Research Fund.

References

[1] Kim D Y and Steckl A J 2010 Electrowetting on paper for electronic paper display *ACS Appl. Mater. Interfaces* **2** 3318–23

[2] Li G, Zhu R and Yang Y 2012 Polymer solar cells *Nat. Photonics* **6** 153–61

[3] Lee H J, Hwang J H, Choi K B, Jung S-G, Kim K N, Shim Y S, Park C H, Park Y W and Ju B-K 2013 Effective indium-doped zinc oxide buffer layer on silver nanowires for electrically highly stable, flexible, transparent, and conductive composite electrodes *ACS Appl. Mater. Interfaces* **5** 10397–403

[4] Fortunato E M C, Barquinha P M C, Pimentel A, Goncalves A M F, Marques A J S, Pereira L M N and Martins R F P 2005 Fully transparent ZnO thin-film transistor produced at room temperature *Adv. Mater.* **17** 590

[5] Banerjee A N, Nandy S, Ghosh C K and Chattopadhyay K K 2007 Fabrication and characterization of all-oxide heterojunction p-$CuAlO_{2+x}$/n-$Zn_{1-x}Al_xO$ transparent diode for potential application in 'invisible electronics' *Thin Solid Films* **515** 7324–30

[6] Lu C-Y, Hsieh K-Y and Liu R 2009 Future challenges of flash memory technologies *Microelectron. Eng.* **86** 283–6

[7] Arimoto Y and Ishiwara H 2004 Current status of ferroelectric randomm-access memory *MRS Bull.* **29** 823–8

[8] Tehrani S, Slaughter J M, Chen E, Durlam M, Shi J and DeHerrera M 1999 Progress and outlook for MRAM technology *IEEE Trans. Magn.* **35** 2814–9

[9] Wong H S P, Raoux S, Kim S, Liang J, Reifenberg J P, Rajendran B, Asheghi M and Goodson K E 2010 Phase change memory *Proc. IEEE* **98** 2201–27

[10] Waser R and Aono M 2007 Nanoionics-based resistive switching memories *Nat. Mater.* **6** 833–40

[11] Waser R, Dittmann R, Staikov G and Szot K 2009 Redox-based resistive switching memories—nanoionic mechanisms, prospects, and challenges *Adv. Mater.* **21** 2632 −+

[12] Sawa A 2008 Resistive switching in transition metal oxides *Mater. Today* **11** 28–36

[13] Breuer T, Siemon A, Linn E, Menzel S, Waser R and Rana V 2015 Low-current operations in 4F(2)-compatible Ta_2O_5-based complementary resistive switches *Nanotechnology* **26** 415202

[14] Li Y, Yuan P, Fu L, Li R, Gao X and Tao C 2015 Coexistence of diode-like volatile and multilevel nonvolatile resistive switching in a ZrO_2/TiO_2 stack structure *Nanotechnology* **26** 391001
[15] Kumar M and Som T 2015 Structural defect-dependent resistive switching in Cu–O/Si studied by Kelvin probe force microscopy and conductive atomic force microscopy *Nanotechnology* **26** 345702
[16] Yeom S-W, Park S W, Jung I-S, Kim M, Ha H J, Shim J H and Ju B-K 2014 Highly flexible titanium dioxide-based resistive switching memory with simple fabrication *Appl. Phys. Express* **7** 101801
[17] Lin C-Y, Wu C-Y, Wu C-Y, Hu C and Tsenga T-Y 2007 Bistable resistive switching in Al_2O_3 memory thin films *J. Electrochem. Soc.* **154** G189–92
[18] Kim S, Nah J, Jo I, Shahrjerdi D, Colombo L, Yao Z, Tutuc E and Banerjee S K 2009 Realization of a high mobility dual-gated graphene field-effect transistor with Al_2O_3 dielectric *Appl. Phys. Lett.* **94** 062107
[19] Carcia P F, McLean R S, Reilly M H, Groner M D and George S M 2006 Ca test of Al_2O_3 gas diffusion barriers grown by atomic layer deposition on polymers *Appl. Phys. Lett.* **89** 031915
[20] Zhang X, Qin J, Xue Y, Yu P, Zhang B, Wang L and Liu R 2014 Effect of aspect ratio and surface defects on the photocatalytic activity of ZnO nanorods *Sci. Rep.* **4** 4596–603
[21] Mao Q, Ji Z and Xi J 2010 Realization of forming-free ZnO-based resistive switching memory by controlling film thickness *J. Phys. D: Appl. Phys.* **43** 395104
[22] Sze S M 1981 *Physics of Semiconductor Devices* 2nd edn (New York: Wiley)
[23] Chang W-Y, Lai Y-C, Wu T-B, Wang S-F, Chen F and Tsai M-J 2008 Unipolar resistive switching characteristics of ZnO thin films for nonvolatile memory applications *Appl. Phys. Lett.* **92** 022110
[24] Kim M J, Jeon D S, Park J H and Kim T G 2015 Bipolar resistive switching characteristics in tantalum nitride-based resistive random access memory devices *Appl. Phys. Lett.* **106** 203101
[25] Mundle R, Terry H, Bahoura M and Pradhan A K 2013 Ozone-assisted atomic layer deposited ZnO thin films for multifunctional device applications *J. Phys. D: Appl. Phys.* **46** 475101
[26] Kim K M, Jeong D S and Hwang C S 2011 Nanofilamentary resistive switching in binary oxide system; a review on the present status and outlook *Nanotechnology* **22** 254002
[27] Na-Phattalung S, Smith M F, Kim K, Du M H, Wei S H, Zhang S B and Limpijumnong S 2006 First-principles study of native defects in anatase TiO_2 *Phys. Rev.* B **73** 125205
[28] Janousch M, Meijer G I, Staub U, Delley B, Karg S F and Andreasson B P 2007 Role of oxygen vacancies in Cr-doped $SrTiO_3$ for resistance-change memory *Adv. Mater.* **19** 2232–5